Lateral length scales of latent image roughness as determined by off-specular neutron reflectivity

Kristopher A. Lavery,[1] Vivek M. Prabhu,[1] Eric K. Lin,[1] Wen-li Wu,[1,a)] Sushil K. Satija,[2] Kwang-Woo Choi,[3] and Matthew Wormington[4]

[1]*Polymers Division, National Institute of Standards and Technology, Gaithersburg, Maryland 20899, USA*
[2]*Center for Neutron Research, National Institute of Standards and Technology, Gaithersburg, Maryland 20899, USA*
[3]*Intel Corporation, Santa Clara, California 95054, USA*
[4]*Bede Scientific Inc., Englewood, Colorado 80112, USA*

A combination of specular and off-specular neutron reflectometries was used to measure the buried lateral roughness of the reaction-diffusion front in a model extreme ultraviolet lithography photoresist. Compositional heterogeneities at the latent reaction-diffusion front has been proposed as a major cause of line edge roughness in photolithographic features. This work describes the experimental observation of the longitudinal and lateral compositional heterogeneities of a latent image, revealing the buried lateral length scale as well as the amplitude of inhomogeneity at the reaction-diffusion front. These measurements aid in determining the origins of line edge roughness formation, while exploring the material limits of the current chemically amplified photoresists. © 2008 American Institute of Physics. [DOI: 10.1063/1.2841663]

The ability to form lithographic features exhibiting line-edge roughness (LER) below 2 nm is a major challenge in the formation of sub-32-nm lithographic features.[1] In an effort to understand the material and processing origins of LER, a great deal of research has been directed at comprehending the impact of exposure,[2–4] latent image formation,[5,6] and development[7–9] on roughness formation. It has been surmised that all of these steps can influence the LER of developed features, although the individual contributions from each of these interdependent processing steps are poorly understood. In particular, the reaction step, in which activated photoacid molecules catalyze reactions in the exposed regions of the photoresist, has been linked to roughness formation through diffusion of acid molecules into unexposed areas.[10–14] Here, we present the first direct measurement of the composition distribution both across and parallel to a reaction-diffusion front in a photoresist film. These measurements will provide crucial insight into the role of the reaction-diffusion process in determining the material limits of LER in lithographic features.

In this work, a model extreme ultraviolet lithography (EUVL) photoresist copolymer is used in a polymer-polymer bilayer geometry that mimics an ideal exposure line edge.[15,16] The bottom layer is a polymer loaded with photoacid generator (PAG) molecules, which acts as the exposed portion of the film. The top layer is the photoresist copolymer in which the protecting group was deuterated to provide neutron scattering length density contrast between protected and deprotected forms of the resist. Bilayer thin films of poly(hydroxystyrene-*co*-d$_9$-tert-butyl acrylate) (PHOST-*co*-d$_9$-TBA) on poly(hydroxyladamantyl methacrylate) (PHAdMA) were prepared on 76.2 mm (3 in.) diameter by 5 mm (0.197 in.) thick float glass substrates using subsequent spin coating steps, as described previously.[16] The PHAdMA bottom layer contained 6% by mass of triphenyl-

sulfonium perfluorobutane sulfonate photoacid generator. Postapply bake steps were performed at 130 °C for 60 s to remove residual solvent. This initial, unexposed bilayer film was characterized using specular and off-specular neutron reflectivity, as described below. The same bilayer film was then exposed to a broadband 248 nm light for 10 s (Oriel Instruments), resulting in a dose of 2.6 mJ/cm^2 and postexposure baked (PEB) at 90 °C for 180 s. Specular and off-specular neutron reflectivity measurements were then completed in an identical manner to the unexposed bilayer.

Specular and off-specular reflectivity measurements were performed at the NIST Center for Neutron Research on the Advanced Neutron Diffractometer/Reflectometer (AND/R) beam line.[17] The neutron wavelength (λ) was 5.00 Å with a wavelength divergence ($\Delta\lambda/\lambda$) of 0.02. Specular measurements were done over a Q_z range of 0.012–0.120 Å^{-1}, where $Q_z = (4\pi/\lambda)\sin(\theta)$ and θ is the specular angle of reflection. Fits to the data were calculated using NIST REFLFIT software[18] to determine the interfaces width σ_{spec}.

During the PEB step, the photoacids in the PHAdMA layer diffuse into the photoresist layer, catalyzing deprotection reactions. The *t*-butyl protecting groups are deuterium labeled, thus allowing the direct observation of the deprotection reaction-diffusion front propagation using neutron reflectometry. Specular neutron reflectometry measurements were done to determine the shape and spatial extent of the reaction-diffusion front. Shown in Fig. 1 is the deprotection front, both before and after PEB. The deprotection extent was calculated from the scattering length density profile, which was determined from fits to the reflectivity curves. The reaction-diffusion front width σ_{spec} was found to be 79 Å, determined from the measured interfacial width of the reacted sample minus the initial bilayer interfacial width. This result was consistent with observations from our previous measurements on the same photoresist copolymer,[16] where the reaction front shape was modeled as an exponen-
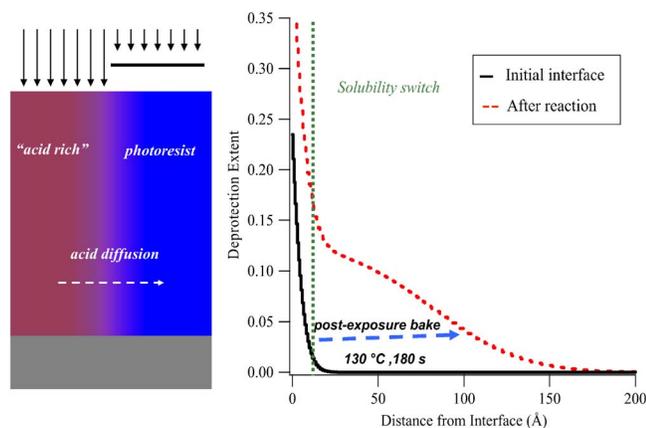
---

a)Electronic mail: wenli@nist.gov.

FIG. 1. (Color online) Polymer bilayer reaction front interface before (solid curve) and after (dashed curve) PEB. Curves were calculated from fits to the specular neutron reflectometry data. The vertical dotted line represents the degree of deprotection beyond which PHOST-*co*-d$_9$ TBA becomes soluble in 0.26N tetramethylammonium hydroxide.

tial decay close to the initial interface followed by a Gaussian function near the advancing front.

Specular reflectometry can measure the depth profile of thin films with nanometer-scale sensitivity in terms of material density and interfacial roughness.[19] However, no information is provided with regards to the lateral length scales because the scattering vector is directed normal to the plane of the substrate. For example, there is no differentiation between a gradient in material density with depth and physical roughness or lateral inhomogeneity. The off-specular neutron reflectometry[20–25] method can address these measurement challenges by examining the diffuse scattering around the specular peak, combining scattering perpendicular (Q_z) and parallel (Q_x in the plane of the beam) to the substrate. Off-specular transverse scans were performed at two different Q_z values, 0.022 and 0.055 Å^{-1}, which provide sensitivity to lateral length scales from $\approx$1000 Å to several micrometers. While Q_z remains largely constant during the transverse scans, Q_x is defined as $(2\pi/\lambda)[\cos(2\theta-\omega)-\cos(\omega)]$, where λ is the neutron wavelength, 2θ is the scattering angle, and ω is the angle of incidence.

The diffuse scattering was analyzed using a modified distorted-wave Born approximation, as described previously.[21,24] This description models the rough interface as self-affine with a roughness amplitude of σ, a lateral length scale of ξ, and a Hurst parameter H. This picture was extended by Wormington *et al.*[24] to include the diffuse scattering from multilayer stacks. Additionally, they separated contributions to the interfacial width arising from a gradient in material density (σ_G) from physical roughness (σ_R). Assuming these terms are not coupled, they can be related to the interfacial width obtained from specular reflectometry through the relation $\sigma_{\text{spec}}^2=\sigma_G^2+\sigma_R^2$. This provides a means to separate the gradual change in the deprotection extent from lateral inhomogeneities at the reaction front.

The off-specular transverse scans, taken before and after reaction, are shown in Fig. 2 along with fits using the model described above. Some qualitative features, such as the intensity between the specular and Yoneda peaks and the intensity in the region immediately adjacent to the specular peak, change slightly after reaction. Figure 2 appears to indicate that the sample roughness decreased upon reaction as evident from the intensity near the specular position. This
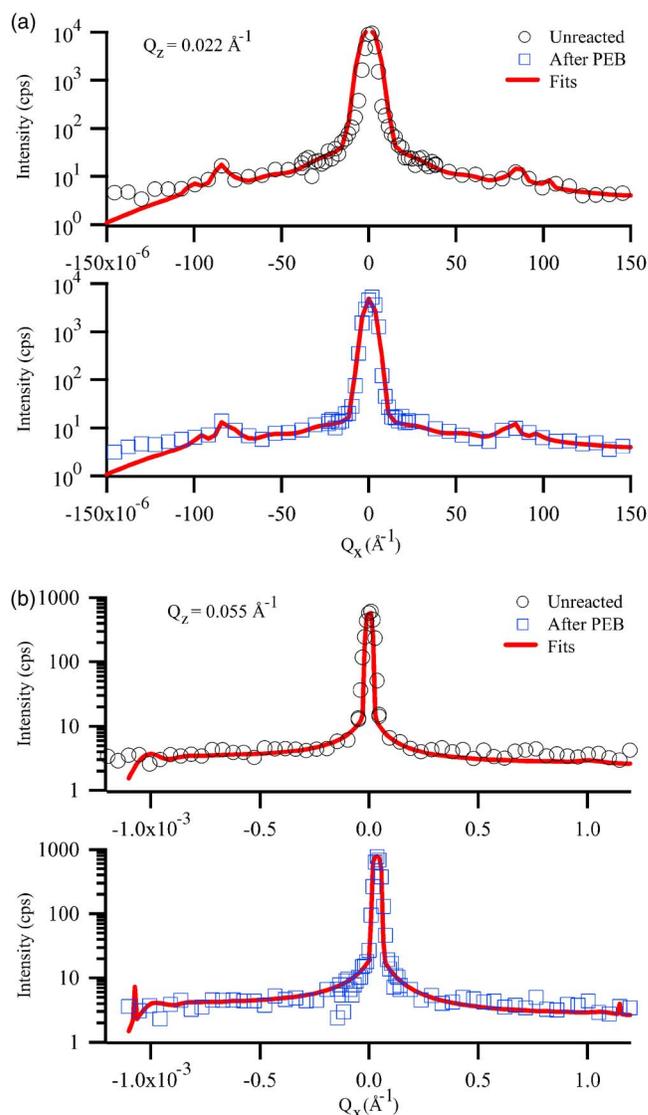

FIG. 2. (Color online) Off-specular transverse curves taken before and after PEB reaction at Q_z values of (a) 0.022 Å^{-1} and (b) 0.055 Å^{-1}. Fits are solid curves through the data.

apparent decrease in roughness upon reaction is largely caused by an increase in the width of the reaction front; from a step function to one with a 79 Å width. In order to quantify the interplay between interface width and roughness, the fitting parameters were systematically changed to obtain the most reliable fit to the data. Figure 3 shows calculations of the diffuse scattering compared to data taken after PEB at a Q_z of 0.022 Å^{-1}. If the entire 79 Å interfacial width is modeled by a lateral compositional inhomogeneity, the result (dotted curve) overestimates the diffuse scattering intensity. In the other extreme, if the reaction front is modeled as a smooth reaction gradient without any lateral compositional inhomogeneity, the result (dashed curve) underestimates the diffuse scattering. The best fit was obtained by a combination of these extremes whereby a lateral compositional inhomogeneity was added at the leading edge of the reaction front while the backend or the region with high degree of reaction stays laterally smooth. The result, shown as the solid curve in Fig. 3, is calculated with a combination of a smooth 75 Å wide compositional gradient and a 25 Å amplitude roughness superimposed at the leading edge of the reaction front. In all cases, H was kept fixed at 0.3. The dotted line in Fig.
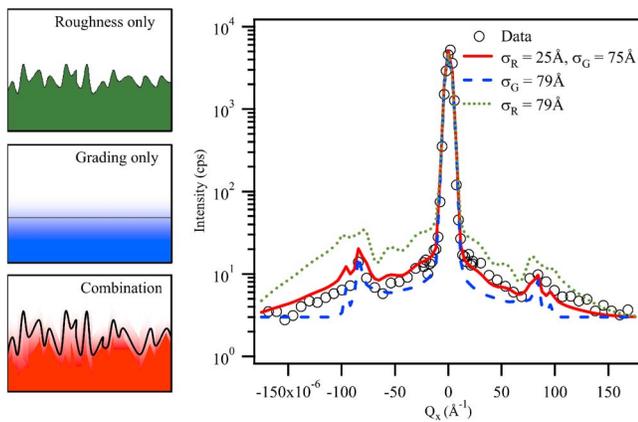
FIG. 3. (Color online) Off-specular transverse scan at Q_z of 0.022 Å^{-1} with calculations for a rough interface (dotted), a smooth gradient interface (dashed), and a combination of the above two (solid).

1 marks the depth where the deprotection level is at 0.2. For P(HOST-*co*-d$_9$-TBA) to dissolve in 0.26 mol/L tetramethylammonium hydroxide (TMAH), which is a typical base developer used in lithographic processing, the deprotection level has to be 0.2 or above.

The lateral length scale (ξ) of the compositional inhomogeneity is estimated by comparing the experimental results to the theoretical curves calculated with different values of ξ, as shown in Fig. 4. At ξ equal to 8000 Å the calculated result fits well not only the diffuse scattering around the specular peak but also the intensity of the Yoneda peak. For the initial bilayer before reaction, the value of ξ is 15 000 Å. A lateral correlation length of 8000 Å is considered to be very large in semiconductor applications where the relevant length scale is between 500 and 2000 Å.

Off-specular reflectivity provides a complete picture of the buried deprotection reaction-diffusion front in a model EUVL photoresist copolymer. These measurements show the latent image possesses a low-amplitude, low-frequency inhomogeneity or roughness at the tip of the reaction wave front. This inhomogeneity occurs at a depth beyond the solubility
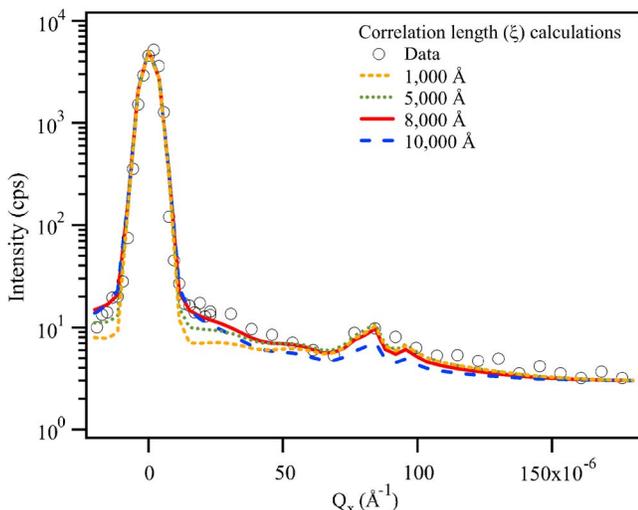
switch for the resist in 0.26 mol/l TMAH, which may diminish the role it plays in roughness formation. Instead, other processes in lithographic feature formation, such as the swelling and deswelling that occur during development, may play more of a role in determining feature quality. Measurements of the lateral length scales at the solid-fluid interface during development will be key in understanding this effect.

Certain commercial equipment and materials are identified in this paper in order to specify adequately the experimental procedure. In no case does such identification imply recommendations by the National Institute of Standards and Technology nor does it imply that the material or equipment identified is necessarily the best available for this purpose.

FIG. 4. (Color online) Off-specular transverse scan at Q_z of 0.022 Å^{-1} with calculations of the diffuse scattering of various correlation length ξ.

[1]D. He and F. Cerrina, J. Vac. Sci. Technol. B **16**, 3748 (1998).
[2]W. D. Hinsberg, F. A. Houle, J. Hoffnagle, M. I. Sanchez, G. Wallraff, M. Morrison, and S. Frank, J. Vac. Sci. Technol. B **16**, 3689 (1998).
[3]A. Pawloski, A. Acheta, H. Levinson, T. B. Michaelson, A. Jamiesin, Y. Nishimura, and C. G. Willson, J. Microlithogr., Microfabr., Microsyst. **5**, 023001 (2006).
[4]J. Shin, G. Han, Y. Ma, K. Moloni, and F. Cerrina, J. Vac. Sci. Technol. B **19**, 2890 (2001).
[5]G. W. Reynolds and J. W. Taylor, J. Vac. Sci. Technol. B **17**, 334 (1999).
[6]J. Shin, Y. Ma, and F. Cerrina, J. Vac. Sci. Technol. B **20**, 2927 (2002).
[7]F. A. Houle, W. D. Hinsberg, and M. I. Sanchez, Macromolecules **35**, 8591 (2002).
[8]F. A. Houle, W. D. Hinsberg, and M. I. Sanchez, J. Vac. Sci. Technol. B **22**, 747 (2004).
[9]P. C. Tsiartas, L. W. Flanagin, C. L. Henderson, W. D. Hinsberg, I. C. Sanchez, R. T. Bonnecaze, and C. G. Willson, Macromolecules **30**, 4656 (1997).
[10]H. Ito, J. Polym. Sci., Part A: Polym. Chem. **41**, 3863 (2003).
[11]C. G. Willson, H. Ito, J. Frechet, T. Tessier, and F. Houliham, J. Electrochem. Soc. **133**, 181 (1986).
[12]H. Ito, Adv. Polym. Sci. **172**, 37 (2005).
[13]G. M. Wallraff and W. D. Hinsberg, Chem. Rev. (Washington, D.C.) **99**, 1801 (1999).
[14]F. A. Houle, W. D. Hinsberg, M. I. Sanchez, and J. A. Hoffnagle, J. Vac. Sci. Technol. B **20**, 924 (2002).
[15]E. K. Lin, C. L. Soles, D. L. Goldfarb, B. C. Trinque, S. D. Burns, R. L. Jones, J. L. Lenhart, M. Angelopoulos, C. G. Willson, S. K. Satija, and W. L. Wu, Science **297**, 372 (2002).
[16]K. A. Lavery, B. D. Vogt, V. M. Prabhu, E. K. Lin, W. L. Wu, S. K. Satija, and K.-W. Choi, J. Vac. Sci. Technol. B **24**, 3044 (2006).
[17]J. A. Dura, D. J. Pierce, C. F. Majkrzak, N. C. Maliszewskyj, D. J. McGillivray, M. Losche, K. V. O'Donovan, M. Mihailescu, U. Perez-Salas, D. L. Worcester, and S. H. White, Rev. Sci. Instrum. **77**, 074301 (2006).
[18]P. A. Kienzle, K. V. O'Donovan, J. F. Ankner, N. F. Berk, and C. F. Majkrzak, http://www.ncnr.nist.gov/reflpak (2006).
[19]T. P. Russell, Mater. Sci. Rep. **5**, 171 (1990).
[20]L. Nevot and P. Croce, Rev. Phys. Appl. **15**, 761 (1980).
[21]S. K. Sinha, E. B. Sirota, S. Garoff, and H. B. Stanley, Phys. Rev. B **38**, 2297 (1988).
[22]W. L. Wu, J. Chem. Phys. **98**, 1687 (1993).
[23]V. Holy and T. Baumbach, Phys. Rev. B **49**, 10668 (1994).
[24]M. Wormington, I. Pape, T. P. A. Hase, B. K. Tanner, and D. K. Bowen, Philos. Mag. Lett. **74**, 211 (1996).
[25]Y. Yoneda, Phys. Rev. **131**, 2010 (1963).